PNAS

Supporting Information for
WUSCHEL-D1 upregulation enhances grain number by inducing formation of multi-ovary producing florets in wheat

Adam Schoen[1†], Guilherme V. Yoshikawa[2†], Parva Kumar Sharma[1], Alex Mahlandt[1], Yi Chen[3], Huajin Sheng[4], Leon Kochian[4], Peng Gao[5], Daoquan Xiang[6], Teagen D. Quilichini[7], Prakash Venglat[4], Sheng Wang[8], Inderjit Singh Yadav[9], Robert Sablowski[10], Yuqi Wang[11], Peng Zhang[11], Annabel Whibley[12], Amy Hill[12], Yong Gu[13], Daniel Rodriguez-Leal[1], Weifeng Luo[1], Yiping Qi[1], Nathan Meier[14], Anmol Kajla[1], Matthew Willman[15], Gina Brown-Guedira[16], Sheron A Simpson[17], Ramey C. Youngblood[17], Amanda Hulse-Kemp[18], Angus Murphy[1], Bikram Gill[19], Cristobal Uauy[3], Raju Datla[8], Nidhi Rawat[1], Scott A. Boden[2*], Vijay Tiwari[1*]

Corresponding authors
Vijay Tiwari, vktiwari@umd.edu
Scott Boden, scott.boden@adelaide.edu.au

This PDF file includes:

Supporting Text 1-5
Figures S1 to S10
Tables S1 to S6

Supplementary Text-1

Method for PacBio based genome assembly: The assembled MOV genome was scaffolded using RagTag (v2.1.0) using *Triticum aestivum* cv. Kariega as reference[1] (Bioproject: PRJNA1221919). The contig level assembly was aligned to the Chinese Spring RefSeq v.1.0 reference genome using minimap2[2]. It was found that a single contig (Mov_ptg000222l, 22.7 Mb) contained our entire mapping interval. Dotplot was constructed using Chromiester between the identified contig and the Chinese Spring RefSeq v.1.0 region 587-592 Mb[3].

Method for Nanopore based assembly of targeted Mov-1 region: Reference data were downloaded from Ensembl Plants release 59 (May 2024): Chinese Spring (IWGSC, GCA_900519105.1); Mace (PGSBv2.1, GCA_903994175.1); Jagger (PGSBv2.1, GCA_903993795.1) and Cadenza (EIv1.1; GCA_902810645.1). The target interval was delimited in reference sequences by BLASTn[4] searches of the coding sequences of predicted genes within the target and flanking regions. The enrichment intervals were Chinese Spring: 2D:565000000-620000000; Mace:2D:562000000-617000000 and Jagger: 2D: 2D:583180000-643190000. The Cadenza assembly was not scaffolded to chromosome level, and 512 scaffolds comprising a total of 56.1 Mb were included in the enrichment template. After sequencing, reads were rebase-called using the super accurate model (dna_r10.4.1_e8.2_400bps_sup@v5.0.0) in Dorado 0.7.2 and these reads were used for downstream analyses. A total of 38.4 Gb (8.9 M reads) was obtained for barcode 20 [MOV] and 34.5Gb (7.1M reads) for barcode 22 [SOV]. Mapping to references was performed using minimap2[267] (version 2.28) in lr:hq mode and alignments were processed using SAMtools[5] (version 1.19). The reads were aligned to the Mace genome and visualized on IGV v2.18.2 for analysis of the target region.

Supplementary Text-2

Method for RNA-seq based transcriptome analysis of developing inflorescences: For RNA-seq transcriptome analysis of developing inflorescences, samples were collected from inflorescences at the vegetative, single ridge, double ridge, lemma primordium and terminal spikelet stages. Total RNA was extracted using the RNeasy Plant Mini Kit (QIAGEN) and treated with Turbo DNase I (Thermo Fisher Scientific). RNA purity was checked using the NanoPhotometer spectrophotometer (IMPLEN, USA), concentration measured using RNA Broad Range Qubit (Fisher Scientific), and RNA integrity was examined using the RNA Nano 6000 Assay Kit of the Bioanalyzer 2100 system (Agilent Technologies, USA). Library construction and RNA-seq were performed by Novogene (Novogene HK Company Ltd., Hong Kong)[6,7,8]. Sequencing libraries were generated using the NEBNext Ultra RNA Library Prep Kit for Illumina (NEB), and index codes were added to attribute sequences to each sample. For sequencing, clustering of the index-coded samples was performed on the cBot Cluster Generation System using the TruSeq PE Cluster Kit v3-cBot-HS (Illumina, USA).

Reads were aligned to the International Wheat Genome Sequencing Consortium (IWGSC) Chinese Spring gene model index v1.1 and the *cv.* Mace PGSBv2.1 genome assembly [6,7,8]. Read alignment and transcript quantification were performed using kallisto-0.42.3[9] and select read alignments in the *Mov-1* locus were manually verified using hisat2 [10]. Differential gene expression analysis, including targeted analysis of genes on chromosome 2DL, was achieved using the R program Sleuth v0.30.0[11]. Transcripts with a false discovery rate (FDR) adjusted *P* value (*q* value) < 0.05 were considered differentially expressed, and transcripts with a mean abundance of < 0.5 TPM across the three replicates were excluded from further analysis. The resulting normalized expression values (in TPM) from the Sleuth analysis were used to visualize transcript levels in

MOV relative to single-ovary sibling lines. Transcript analysis plots were performed using Visual Studio Code v1.97.2, with R 4.4.1. Transcript values of *WUS-A1*, *WUS-B1* and *WUS-D1* from MOV and SOV were plotted with ggplot2_3.5.1 using data obtained from reads aligned to cv. Mace genome. Relative expression values were plotted against the Chinese Spring genome to highlight the positions of transcripts that were up or downregulated in MOV, using the karyoploteR_1.32.0 package.

Method for RNA-seq based transcriptome analysis of developing ovaries: Clean reads were aligned to the Chinese Spring RefSeq v1.0 using HISAT2 software using default parameters[10]. SAM files were converted to BAM files and low-quality alignments were filtered using samtools[12]. Read counts were determined using RSubread software v. 2.16.1 using the featureCounts function and tpm and rpkm values were calculated using edgeR software v.3.42.4[13,14]. Differential expression between CS and MOV was calculated using DESeq2[15].

Supplementary Text-3

Phylogenetic Tree Construction: The predicted protein sequence of WUS-D1 was used to perform Basic Local Alignment Search Tool (BLAST) on Uniprot (https://www.uniprot.org/), Plant Transcription Factor Database (https://planttfdb.gao-lab.org/), EnsemblPlants (https://plants.ensembl.org/), and GrainGenes (https://wheat.pw.usda.gov/GG3/) to identify homologous protein sequences. Protein sequences were aligned using Multiple Alignment using Fast Fourier Transform (MAFFT; NGPhylogeny.fr) and cleaned using Block Mapping and Gathering with Entropy (BMGE) [16-19]. Phylogenetic tree construction was performed using MRBAYES and visualized and edited using Interactive Tree of Life (iTOL) v6 [20,21], and the resultant tree was compared to a similar tree generated for the WOX transcription factors of wheat [35].

Supplementary Text-4

Method for TILLING based gene validation: Several markers were developed to span the length of the *Mov-1* candidate gene (*WUS-D1*) to discover deleterious SNPs within the coding region and tested for specificity. Markers were initially run on the 4x pools, and SNPs were determined by the Cel-1 assay[22]. Positive mutant pools were then deconvoluted to identify individuals harboring SNPs. PCR products from the mutants were purified and Sanger sequenced using the BigDye Terminator v3.1 Cycle Sequencing Kit (Thermo Fisher) and the 3730xl DNA Analyzer (Thermo Fisher). Sequences were aligned to the wild-type sequence using SnapGene v6.1. Mutation effects were calculated using Protein Variation Effect Analyzer (PROVEAN) v1.1 software and Sorting Intolerant from Tolerant (SIFT) software[23,24]. Four mutants with deleterious SIFT and PROVEAN scores were identified and selfed until the M_6 generation to fix any background mutations. Fifteen plants from two subsequent generations (M_6 and M_7) were phenotyped per mutant for ovary number and grain set. Ovary and grain phenotypes were collected from primary florets of six central spikelets per spike.

Supplementary Text-5

Method for MOV Deletion Panel Genotyping using GBS data: Using a modified method described by Singh et al., 2020, DNA was digested with PstI and MspI restriction enzymes, and barcode adaptors were ligated to the digested fragments[25]. Libraries were constructed and sequenced on the NovaSeq 6000 system at a 384-plex level. The reads obtained were demultiplexed, low-quality reads filtered out, and adaptor sequences trimmed using Ultraplex software v.1.2.10. The trimmed reads were aligned to the Chinese Spring reference v.1.0 genome using Bowtie2 v.2.5.3 with the following parameters: --threads 40 -q --end-to-end -D 20 -R 3 -N 0 -L 10 -i S,1,0.25. SAM files were converted to BAM files using Samtools. Coverage for chromosome 2D was calculated with Bedtools v.2.30.0 using the command bedtools coverage with a sliding window of 500 kbp. Coverage data were visualized in R software v.4.3.1. The R5 and R6 generation irradiation mutants were phenotyped in the same way as the EMS mutants.

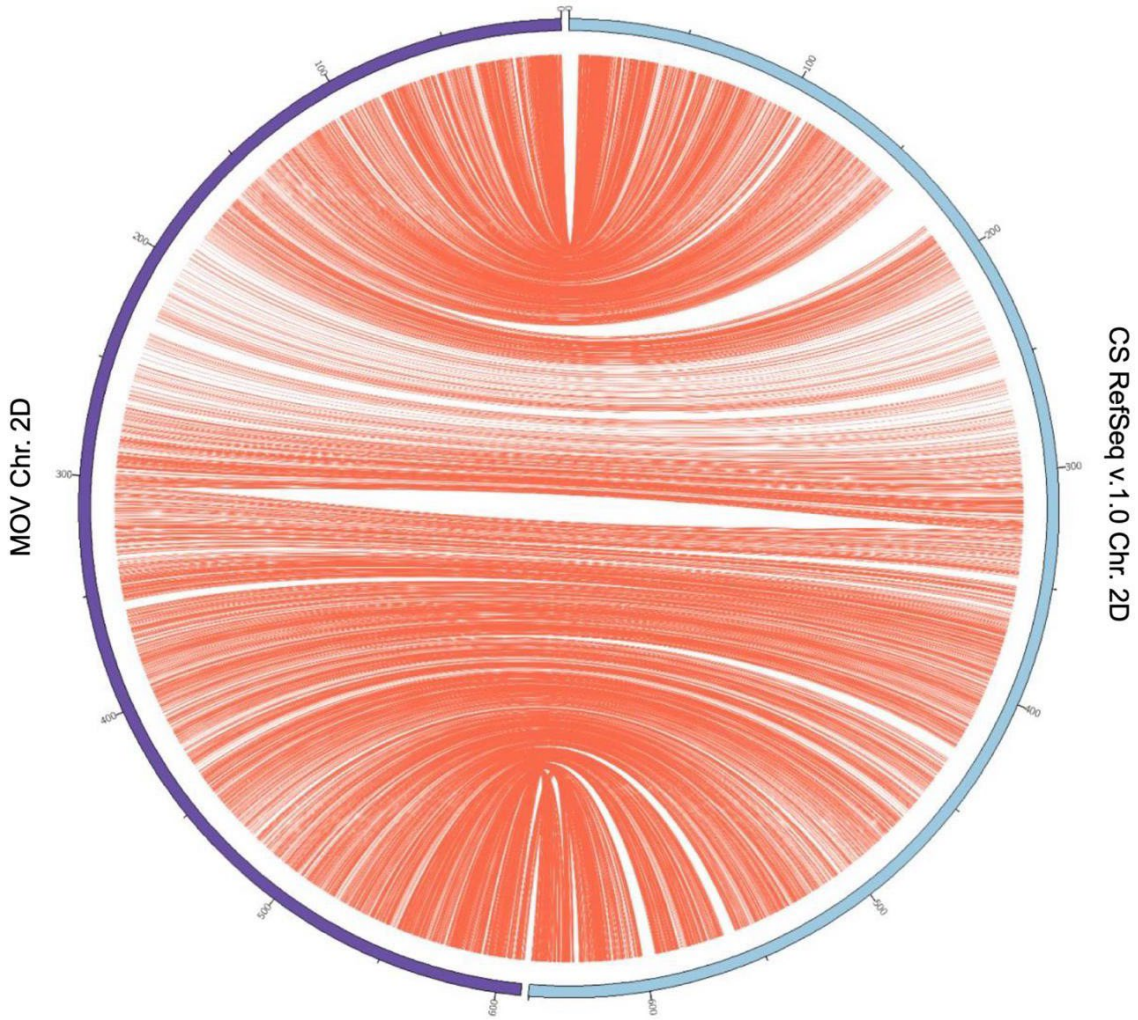

Figure S1. Circos plot showing synteny between MOV and the Chinese Spring RefSeq v.1.0 for chromosome 2D. Red lines indicate synthenic regions of chromosome 2D between Chinese Spring (CS RefSeq; light blue) and MOV (dark blue), with numbers indicating the Mbp position.

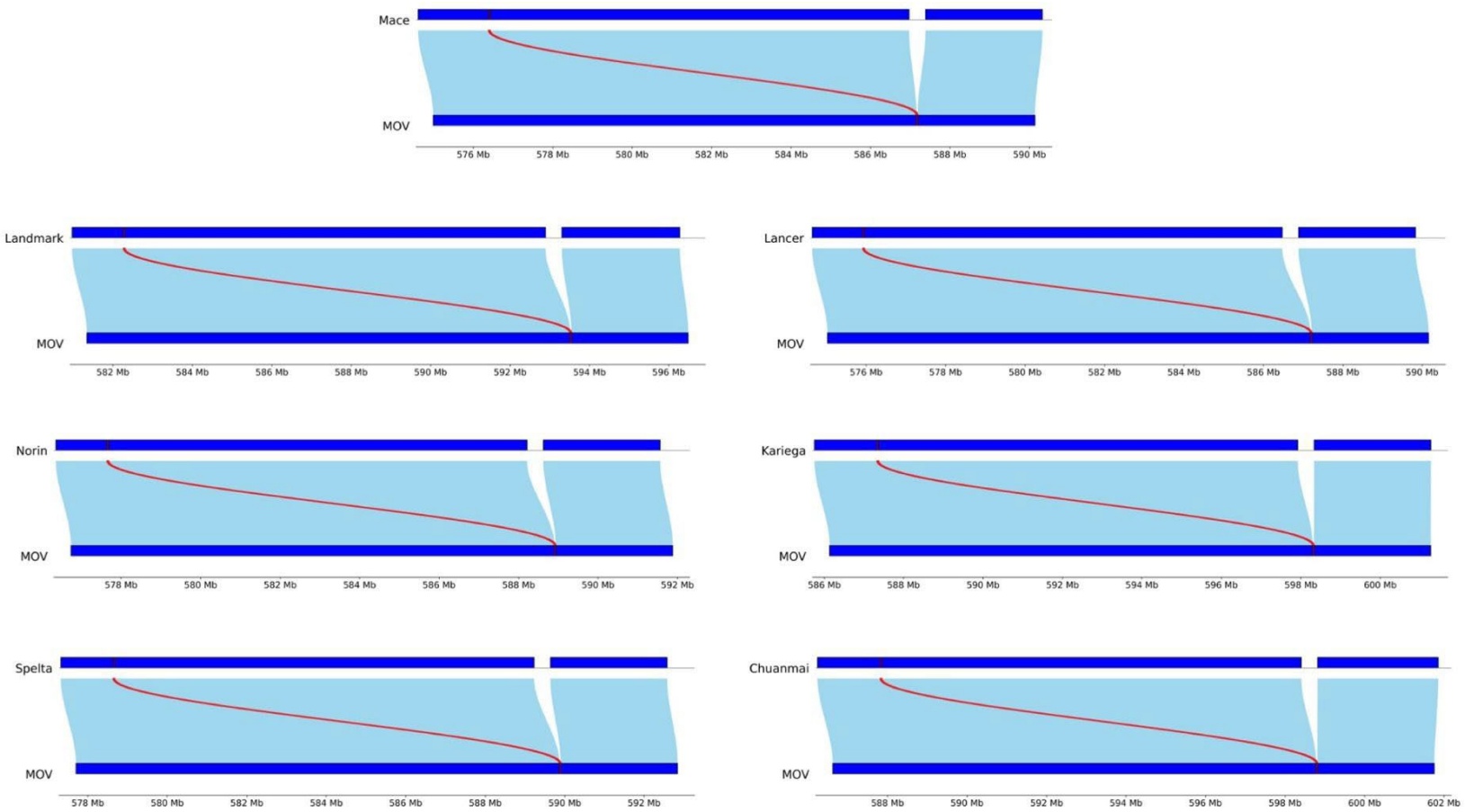

Figure S2. Comparison of *Mov-1* region in MOV to multiple wheat genomes. Seven additional syntenic comparisons showed the deletion of 414 kb region and the 30 kb rearrangement in MOV. Blue lines indicate collinear regions; the red line indicates the inverted translocation event. The x-axis scale shows chromosomal coordinates of the top genotype.

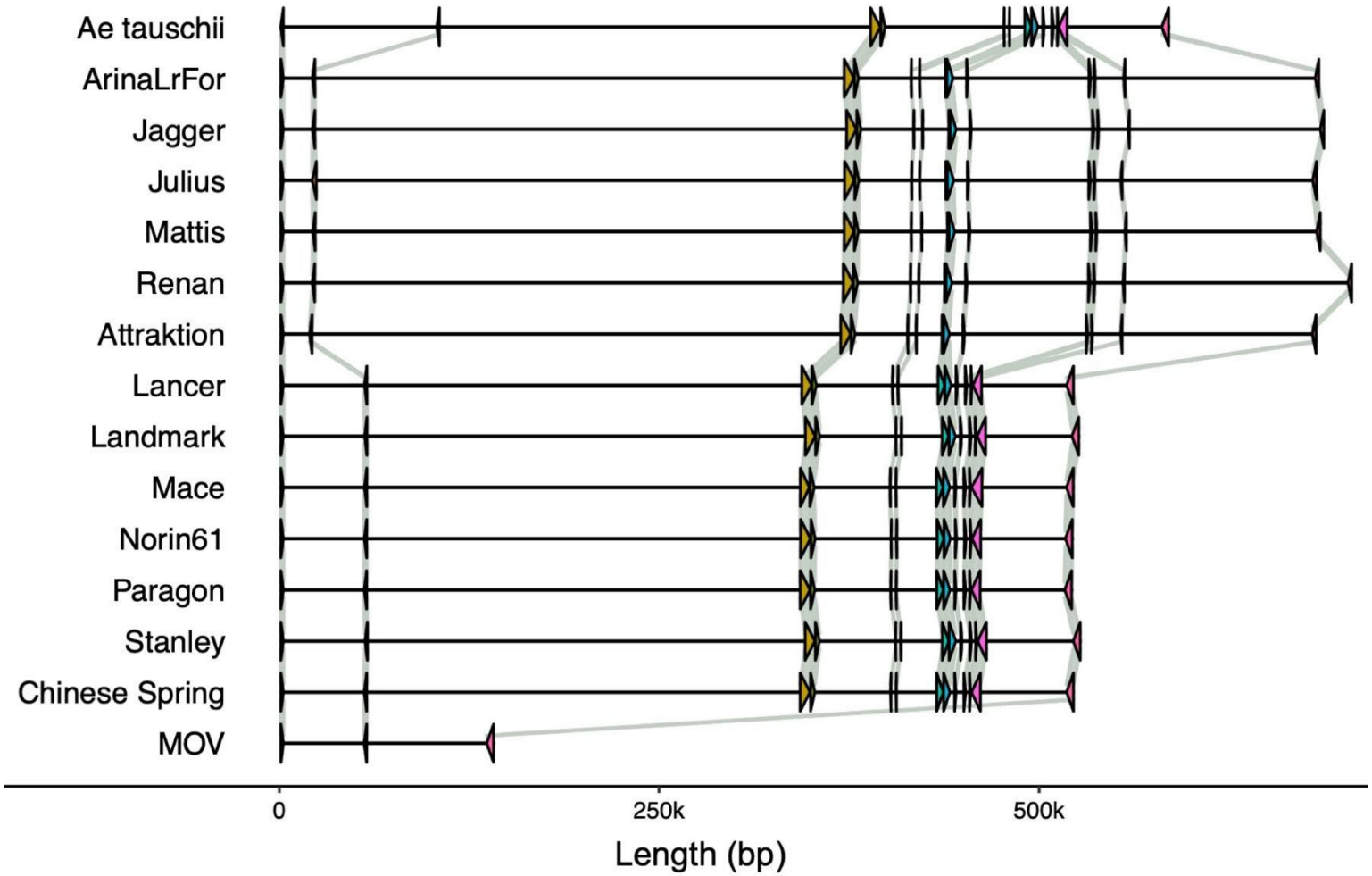

Figure S3. Comparison of the fine-mapping interval in MOV background compared to the 10+ genomes and *Ae. tauschii* .
Alignments of genomic regions for the *Mov-1* locus of chromosome 2D in MOV, relative to *Ae. tauschii* and 13 hexaploid wheat lines. The colored arrows indicate annotated genes, including the 10 deleted genes of *Mov-1*.

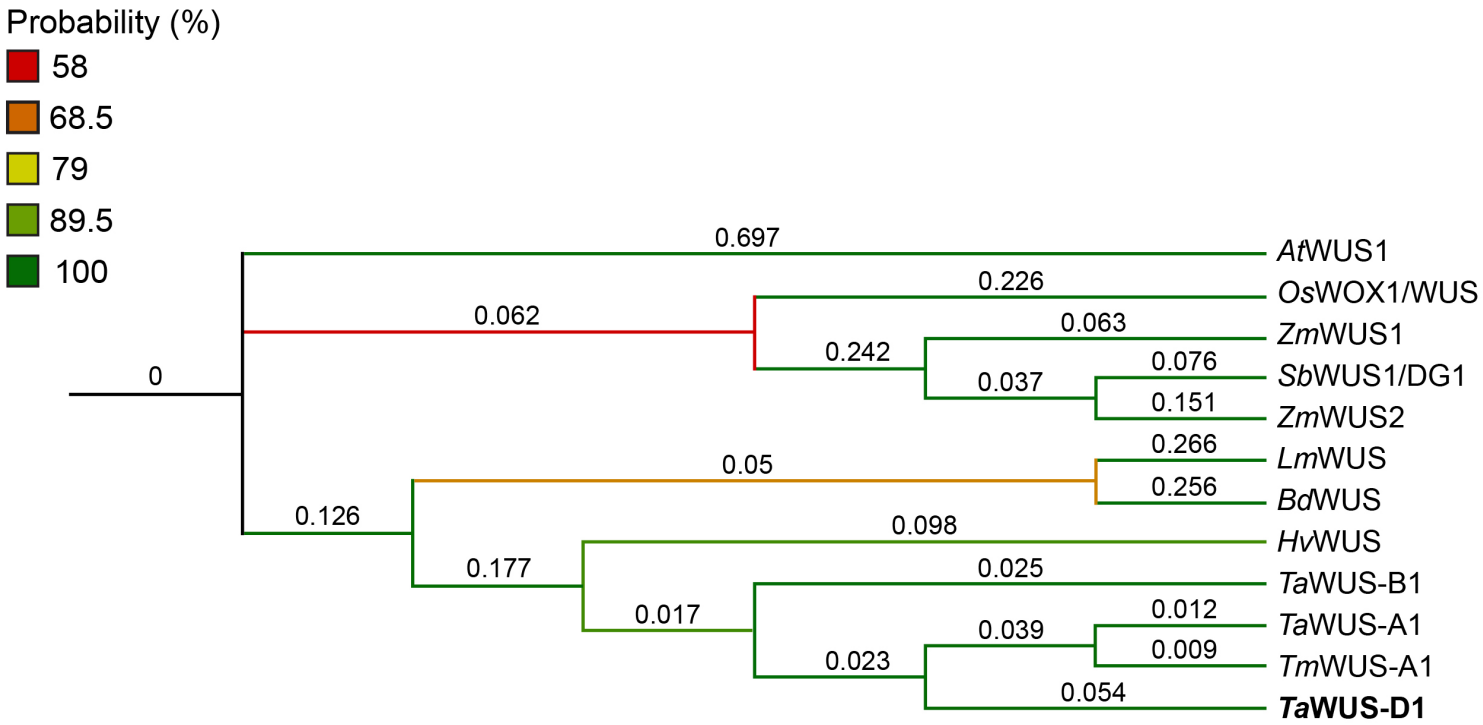

Figure S4. Phylogenetic tree of orthologs of *WUS-D1* in selected plant species. Bayesian phylogenetic tree of WUSCHEL-related homeobox sequences including WUS-D1 from *Triticum aestivum* (*Ta*) and orthologs from selected species. The tree was inferred using MrBayes under a Bayesian framework. The values indicate the branch lengths that represent the expected number of substitutions per site, and the posterior probability values of the clades are color-coded according to the percentage scale (red = lower support; green = higher support). Homeologous copies from hexaploid wheat (*TaWUS-A1, TaWUS-B1*) and *T. monococcum* (*Tm*) are shown for comparison. WUS from *Arabidopsis thaliana* (*At*) is included for outgroup comparison. *Os*, *Oryza sativa*; *Zm*, *Zea mays*; *Sb*, *Sorghum bicolor*; *Lm*, *Lolium multiflorum*; *Bd*, *Brachypodium distachyon*; *Hv*, *Hordeum vulgare*.

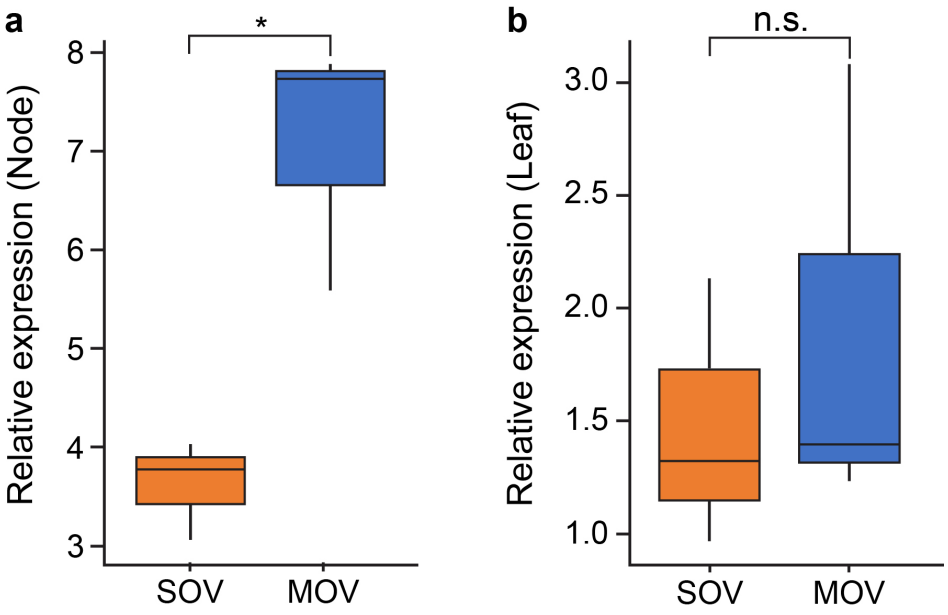

Figure S5. Analysis of *WUS-D1* expression in vegetative tissues. a-b. Droplet digital PCR analysis of *WUS-D1* transcripts in stem node (**a**) and leaf (**b**) tissue of single-ovary (SOV, orange) and multi-ovary (MOV, blue) wheat, showing significant upregulation in stem nodes of MOV ($P < 0.05$, *), but not in leaves. In the boxplots, the box is bound by the upper and lower quartiles, the central bar represents the median and whiskers indicate the maximum and minimum values of three biological replicates.

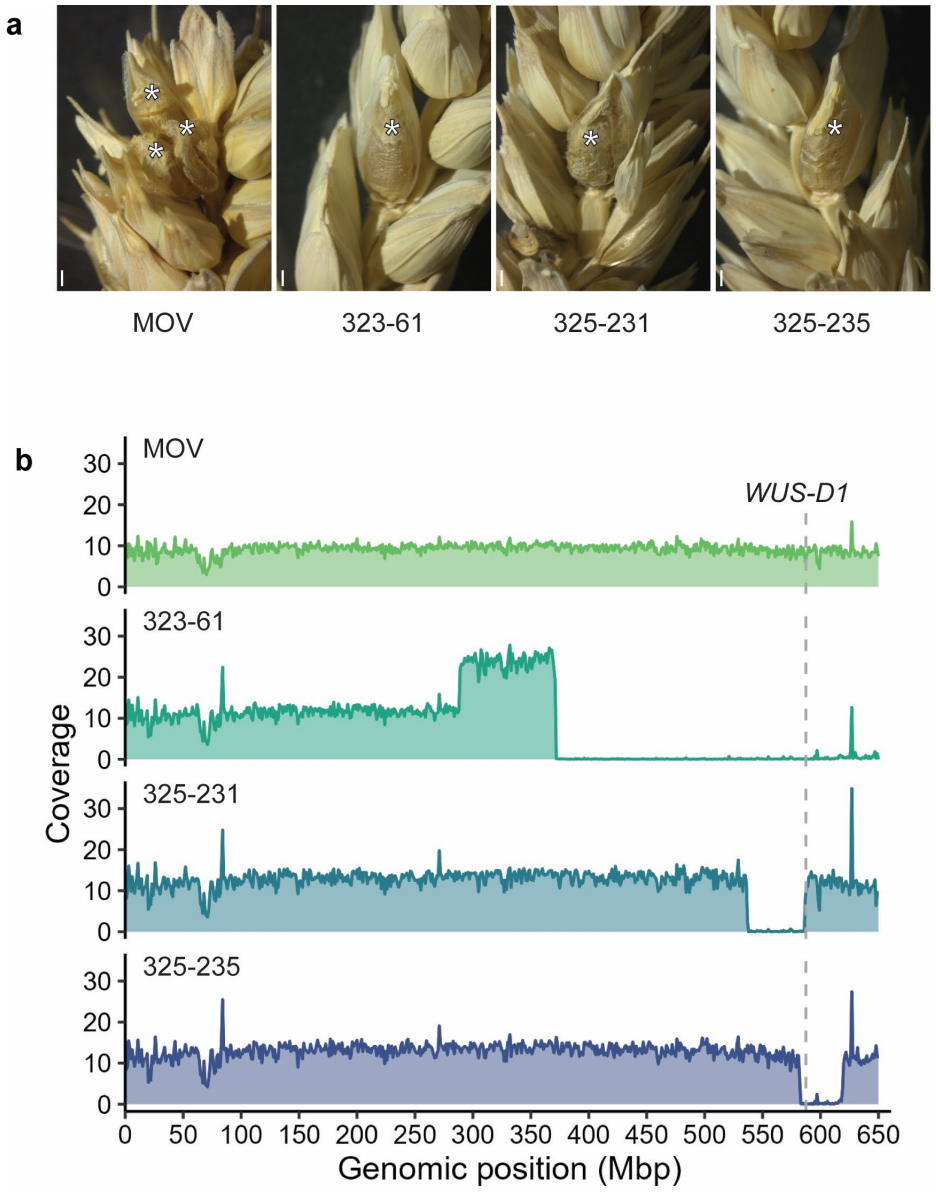

Figure S6. Additional *WUS-D1* deletion mutants found in independent gamma irradiated population showing loss-of-function phenotype. a. Grain set phenotype in MOV and three independent mutants showing loss of the multi-ovary trait. **b.** Plots showing read coverage of long-range sequencing reads across Chromosome 2D in MOV and the three deletion lines: 323-61, 325-231 and 325-235. Positions on x-axis are relative to *cv.* Mace genome, used for alignment, and the dashed grey line indicates the position of *WUS-D1*.

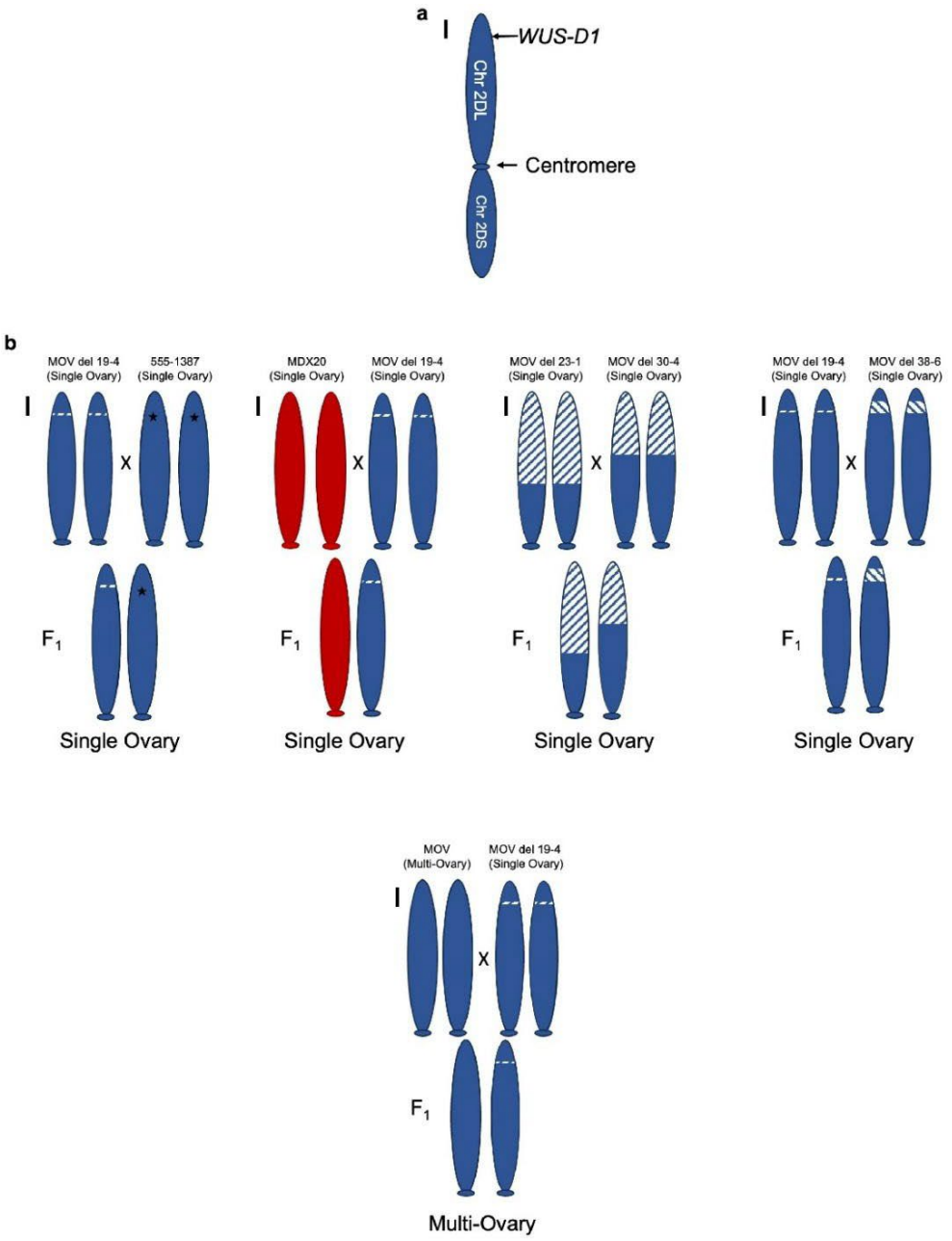

Figure S7. A schematic of the mutant crossing strategy to confirm that *WUS-D1* underlies the *Mov-1* locus. a. A diagram of wheat chromosome 2D, showing the location of the centromere and *WUS-D1* on the long arm. **b.** Diagrams of the different crosses used to validate the effect of mutant *WUS-D1* alleles. Dashes represent deleted regions of the chromosome arm and black stars indicate the location of EMS-induced mutant alleles. Blue indicates the MOV genome content, and red indicates the genome of the winter wheat single ovary line (MDX20). Observed phenotypes of the F_1 progeny are described below each cross. Scale bar, 50 Mbp. The deletion of MOV del 19-4 is expanded slightly to improve visibility.

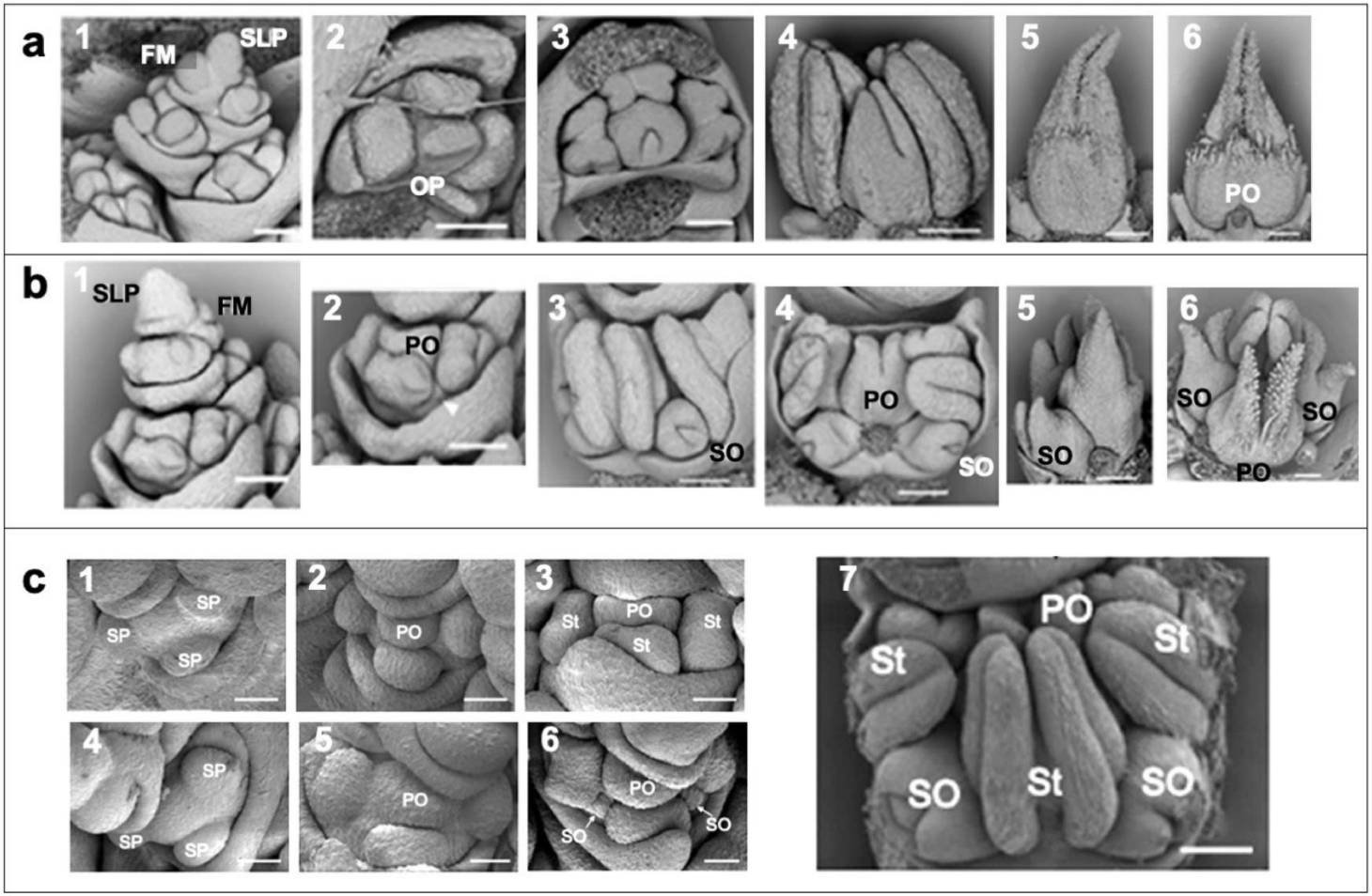

Figure S8. Scanning electron microscopy images capturing the ontogenic sequence of floret and ovary development in SOV and MOV wheat. Chinese Spring wheat line (panel **a**, 1-6) and MOV (panel **b**, 1-6) lines. Panel **c** shows close-up images of the initiation and development of ovary primordia in Chinese Spring (**c**, 1-3) and MOV (**c**, 4-7). The arrowhead in **b**-2 the initiation site of the secondary ovary primordia. All or frontal stamens were removed to image the carpel primordia in panels **a** (4-6) and **b** (4-6). Scale bar, 50 µm. SLP – spikelet primordium; FP – floret primordium; OP – ovary primordium; PO – primary ovary primordium; SO – secondary ovary primordium; SP – stamen primordium; St – stamen.

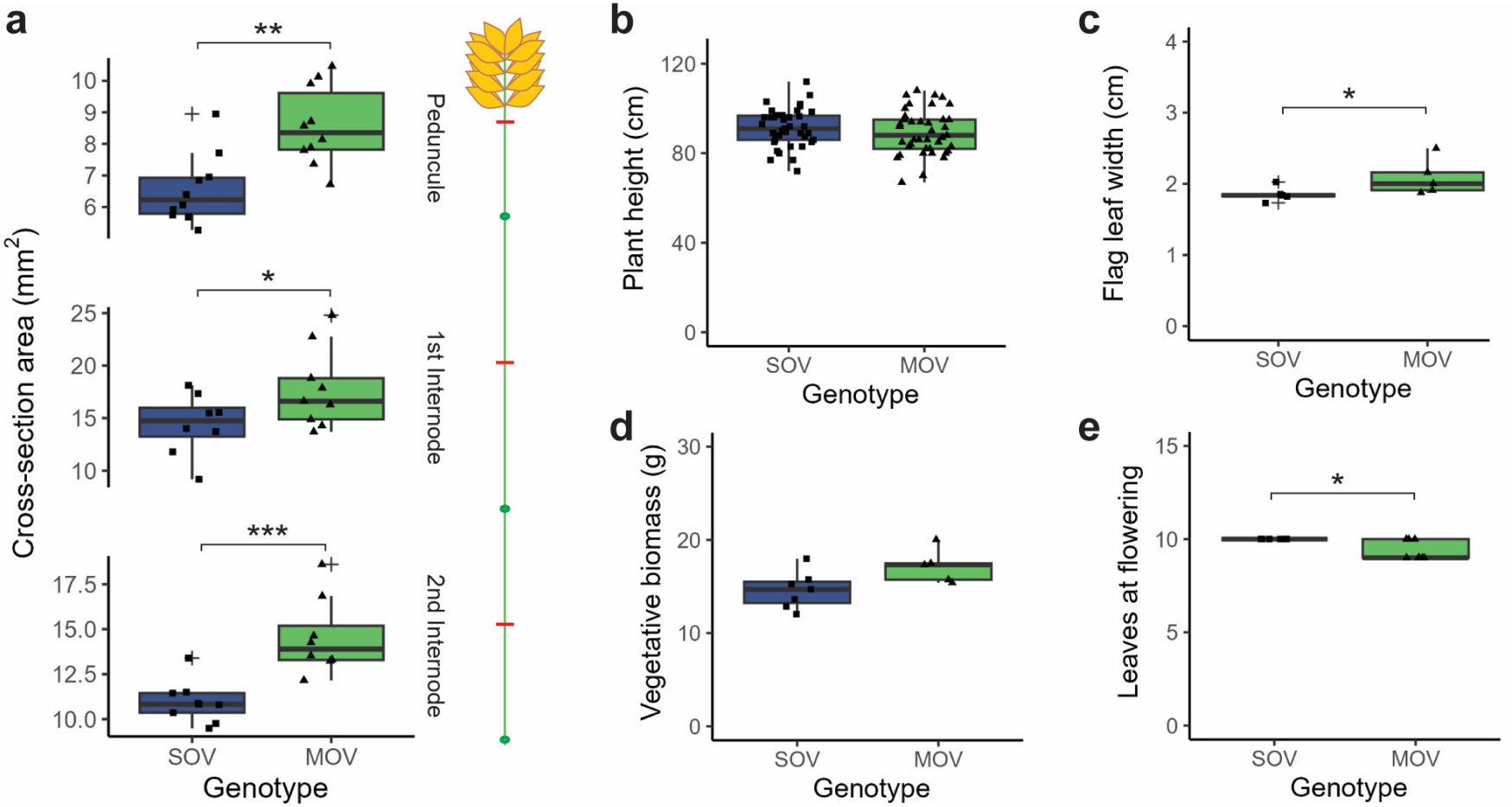

Figure S9 - Analysis of vegetative traits in SOV and MOV NIL plants. a. Cross-sections of the stem at the peduncle of the spike, and of the middle of the first and second internodes, show that the stem of MOV plants is significantly wider than SOV plants. A depiction of the areas cut (in red) is shown next to the graph. **b**. MOV plants did not show a significant difference in height from SOV plants; however, MOV plants showed a small but significant increase in flag leaf width (**c**). **d**. MOV plants showed a slight, but non-significant, increase in dry vegetative biomass. **e**. MOV plants often formed less leaves at maturity, compared to SOV plants. In the boxplots, each box is bounded by the lower and upper quartiles, the central bar represents the median, and whiskers indicate minimum and maximum values of 8-10 (**a**), 39 (**b**), 5 (**c**), or 7 (**d-e**) biological replicates. * $P<0.05$, ** $P<0.01$, *** $P<0.001$(non-parametric Wilcoxon-Mann-Whitney Test).

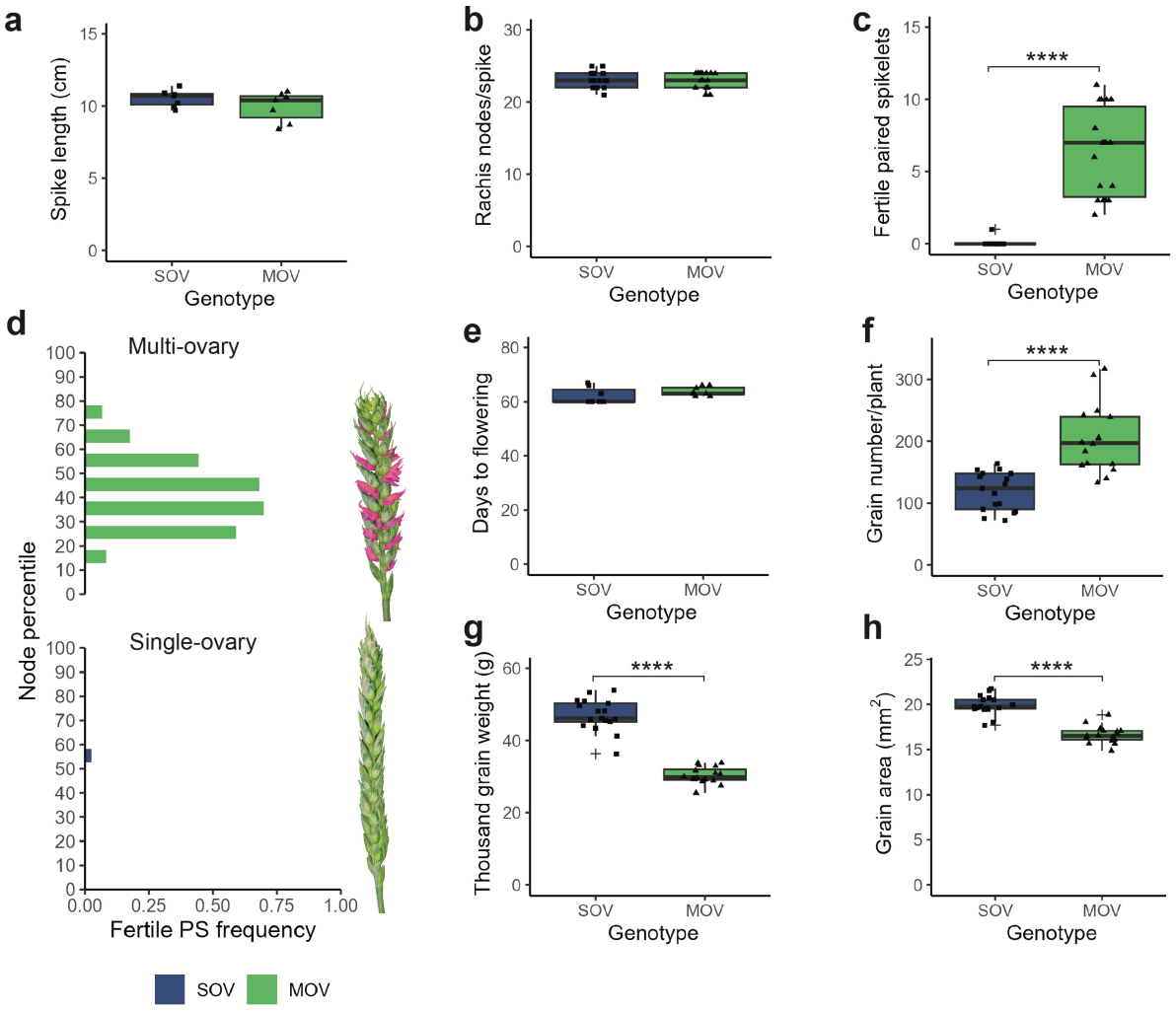

Figure S10 – Summary of flowering and yield-related traits in SOV and MOV plants. Spike length (**a**) and rachis node number per spike (**b**) were not statistically different between the two genotypes. **c**. MOV plants developed significantly more fertile paired spikelets than SOV, which were predominantly distributed in the centre of the spike as shown in (**d**); where secondary spikelets are shaded in pink. **e.** Flowering time was not significantly different between SOV or MOV plants. **f**. MOV plants produced significantly more grains per plant than single-ovary plants, but (**g**) thousand grain weight and (**h**) grain area were significantly higher in SOV plants, compared to MOV. In the boxplots, each box is bounded by the lower and upper quartiles, the central bar represents the median, and whiskers indicate minimum and maximum values of 7 (**a, e**), 18 (**b-d**) or 16 (**f-h**) biological replicates. **** $P < 0.0001$, * $P < 0.05$ (non-parametric Wilcoxon-Mann-Whitney Test).

Supplementary Table 1. Summary statistics of the assembled MOV genome.

Parameter	Value
Total Contigs	2940
Genome Size (Mb)	14479.711
Contig N/L50 (Mb)	241/15.652
Max scaffold length (Mb)	117.889
Complete BUSCOs (%)	99.39
Complete and single-copy BUSCOs (%)	2.82
Complete and duplicated BUSCOs (%)	96.57
Fragmented BUSCOs (%)	0.06
Missing BUSCOs (%)	0.55
Total BUSCO groups searched	4896

Supplementary Table 2. List of investigated Cadenza TILLING mutants for genes within *Mov-1* deletion region. All mutant lines formed florets with one pistil.

Gene ID	Mutant ID	Mutation Type	AA Change
TraesCS2D02G491200	Cadenza0161	missense variant	P/S
	Cadenza0911	missense variant	G/D
	Cadenza0240	missense variant	G/E
	Cadenza1273	missense variant	P/S
	Cadenza0469	missense variant	R/Q
	Cadenza0604	missense variant	H/Y
	Cadenza0474	missense variant	P/S
	Cadenza0630	missense variant	G/E
	Cadenza1715	missense variant	T/I
	Cadenza1677	missense variant	A/V
	Cadenza1070	missense variant	P/L
	Cadenza1599	missense variant	R/C
	Cadenza0348	missense variant	P/L
	Cadenza1517	missense variant	E/K
	Cadenza1270	missense variant	L/S
	Cadenza1443	missense variant	C/Y
	Cadenza0161	missense variant	P/S
	Cadenza0911	missense variant	G/D
	Cadenza0240	missense variant	G/E
	Cadenza1273	missense variant	P/S
	Cadenza0469	missense variant	R/Q
	Cadenza0604	missense variant	H/Y
	Cadenza0474	missense variant	P/S
	Cadenza0630	missense variant	G/E
	Cadenza1715	missense variant	T/I
	Cadenza1677	missense variant	A/V
	Cadenza1070	missense variant	P/L
	Cadenza1599	missense variant	R/C
	Cadenza0348	missense variant	P/L
	Cadenza1517	missense variant	E/K
	Cadenza1270	missense variant	L/S
	Cadenza1443	missense variant	C/Y
TraesCS2D02G491300	Cadenza0155	missense variant	P/L
	Cadenza0553	missense variant	A/V
	Cadenza1392	missense variant	G/E
	Cadenza0899	missense variant	T/I

TraesCS2D02G491600	Cadenza0477	missense variant	G/E
	Cadenza0562	missense variant	N/S
	Cadenza0019	missense variant	N/S
	Cadenza2098	missense variant	N/S
	Cadenza1044	missense variant	N/S
	Cadenza1567	missense variant	N/S
	Cadenza1605	missense variant	N/S
	Cadenza0159	missense variant	N/S
	Cadenza2070	missense variant	N/S
	Cadenza2107	missense variant	N/S
	Cadenza0877	missense variant	N/S
	Cadenza0887	missense variant	N/S
	Cadenza0392	missense variant	N/S
	Cadenza1714	missense variant	N/S
TraesCS2D02G491700	Cadenza1746	missense variant	P/L
	Cadenza1478	missense variant	G/V
	Cadenza0156	missense variant	G/E
	Cadenza0871	stop gained	Q/*
	Cadenza1069	missense variant	R/Q
TraesCS2D02G491800	Cadenza1535	stop gained	L/*
	Cadenza1375	stop gained	L/*
	Cadenza1793	stop gained	L/*
	Cadenza0999	stop gained	L/*
	Cadenza1715	stop gained	L/*
	Cadenza0167	stop gained	L/*
	Cadenza1987	stop gained	L/*
	Cadenza0450	missense variant	A/T
TraesCS2D02G491900	Cadenza1800	missense variant	A/T
	Cadenza0393	missense variant	S/P
	Cadenza0620	missense variant	G/W
	Cadenza1448	missense variant	G/W
	Cadenza1762	missense variant	A/T
	Cadenza1713	missense variant	C/Y
TraesCS2D02G492100	Cadenza1816	missense variant	A/V
	Cadenza1052	missense variant	R/C
	Cadenza0230	missense variant	P/S
	Cadenza1750	missense variant	P/S
	Cadenza0669	missense variant	E/K
	Cadenza1773	missense variant	A/T

Supplementary Table 3. Expression profile of genes within the candidate region during early inflorescence and ovary development.

Transcript ID	MOV				SOV			
	Double Ridge Stage (TPM)	Terminal Spikelet Stage (TPM)	Very Young Ovary (RPKM)	Young Ovary (RPKM)	Double Ridge Stage (TPM)	Terminal Spikelet Stage (TPM)	Very Young Ovary (RPKM)	Young Ovary (RPKM)
TraesCS2D02G491100.1	0 ± 0	0 ± 0	0 ± 0	0 ± 0	0 ± 0	0 ± 0	0 ± 0	0.01 ± 0.02
TraesCS2D02G491200.1	**0 ± 0**	**0 ± 0**	**0 ± 0**	**0 ± 0**	**3.25 ± 0.15**	**0.84 ± 0.08**	**0 ± 0**	**0 ± 0**
TraesCS2D02G491200.2	**0 ± 0**	**0 ± 0**	**0 ± 0**	**0 ± 0**	**1.24 ± 0.04**	**0.31 ± 0.04**	**0 ± 0**	**0 ± 0**
TraesCS2D02G491300.1	**0 ± 0**	**0 ± 0**	**0 ± 0**	**0 ± 0**	**4.60 ± 2.25**	**3.71 ± 0.43**	**29.32 ± 1.34**	**22.86 ± 0.08**
TraesCS2D02G491400.1	**0 ± 0**	**0 ± 0**	**0 ± 0**	**0 ± 0**	**0 ± 0**	**0 ± 0**	**0.30 ± 0.10**	**0.25 ± 0.03**
TraesCS2D02G491500.1	**0 ± 0**	**0 ± 0**	**0 ± 0**	**0 ± 0**	**0 ± 0**	**0 ± 0**	**0 ± 0**	**0 ± 0**
TraesCS2D02G491600.1	**0 ± 0**	**0 ± 0**	**0 ± 0**	**0 ± 0**	**0 ± 0**	**0.01 ± 0.02**	**0.43 ± 0.03**	**0.38 ± 0.11**
TraesCS2D02G491700.1	**0 ± 0**	**0 ± 0**	**0 ± 0**	**0 ± 0**	**0.34 ± 0.17**	**0.22 ± 0.02**	**1.84 ± 0.45**	**2.55 ± 0.00**
TraesCS2D02G491800.1	**0 ± 0**	**0 ± 0**	**0 ± 0**	**0 ± 0**	**0 ± 0**	**0 ± 0**	**0 ± 0**	**0 ± 0**
TraesCS2D02G491900.1	**0 ± 0**	**0 ± 0**	**0 ± 0**	**0 ± 0**	**0 ± 0**	**0 ± 0**	**0.03 ± 0.04**	**0.02 ± 0.02**
TraesCS2D02G492000.1	**0 ± 0**	**0 ± 0**	**0 ± 0**	**0 ± 0**	**0 ± 0**	**0 ± 0**	**0 ± 0**	**0 ± 0**
TraesCS2D02G492100.1	**0 ± 0**	**0 ± 0**	**0 ± 0**	**0 ± 0**	**0 ± 0**	**0 ± 0**	**0.04 ± 0.01**	**0.01 ± 0.02**
TaWUS-D1	23.74 ± 1.91	1.80 ± 0.76	1.46 ± 0.27	0.39 ± 0.07	0.69 ± 0.22	0 ± 0	0.21 ± 0.07	0.12 ± 0.08
TraesCS2D02G492200.1	7.80 ± 0.29	6.67 ± 1.99	4.39 ± 0.19	3.80 ± 0.16	0.86 ± 0.50	0.56 ± 0.45	3.25 ± 1.29	3.79 ± 0.30

Gene IDs in **bold** indicate deleted genes in the *Mov-1* locus. Transcript levels are shown as either transcripts per millon (TPM) or reads per kilobase per million (RPKM), with values representing the mean ± s.e.m. of three biological replicates.

Supplementary Table 4. List of gamma-irradiated mutants and their observed phenotypes

#	Mutant ID	Origin	Phenotype
1	MOV del 19-4	UMD	Single ovary
2	MOV del 30-4	UMD	Single ovary
3	MOV del 23-1	UMD	Single ovary
4	MOV del 1-124	UMD	Single ovary
5	MOV del 38-6	UMD	Single ovary
6	MOV del 40-3	UMD	Single ovary
7	323-61	UA	Single ovary
8	325-231	UA	Single ovary
9	325-235	UA	Single ovary

UMD: University of Maryland, College Park, Maryland, USA

UA: University of Adelaide, Urrbrae, South Australia, Australia

Supplementary Table 5. Crosses used for mutant complementation analysis and their phenotypes

ID	Cross	Generation	Cross Type	Expected Phenotype	Observed Phenotype
1	555-1387/19-4	F_1	EMS/Deletion	Single Ovary	Single Ovary
2	19-4/SOV-WW	F_1	Deletion/SOV	Single Ovary	Single Ovary
3	23-1/30-4	F_1	Deletion/Deletion	Single Ovary	Single Ovary
4	19-4/38-6	F_1	Deletion/Deletion	Single Ovary	Single Ovary
5	19-4/MOV WT	F_1	Deletion/MOV	Multi-Ovary	Multi-Ovary

Supplementary Table 6. List of primers used in this study

#	Primer Name	Forward Sequence (5'-3')	Reverse Sequence (5'-3')	Assay
1	RD_ddpcr_MOV	CCCGGATGCGAGCGCTACT	AAAGGGAAGCCCGCAGCT	In situ PCR, In situ hybridization, ddPCR
2	Ta_Actin	CCACCACAGCACCTACGCCGT	ATGGAAGCTGCTGGAATCCAT	ddPCR
3	Ta_Actin_probe	CCATACAGATCCTTCCTGATATCCACATCACACTTC	N/A	*TaActin* probe +HEX, 100 nm PrimeTime® 5' HEX/ZEN/3' IB®FQ
4	MOV_probe	CCACCACAGCACCTACGCCGT	N/A	MOV ddPCR probe, Eco 2.5nM 5' 6-FAM/ZEN/3' IBFQ
5	mov_2D_580	AGGCTGCAACAAGCCAACAA	CCAACAGCTGCTGACATTCTTC	Deletion Mapping
6	mov_2D_584	GTAGGCCGACCGGATGAA	CGGGCAGATCTCAAGCAA	Deletion Mapping
7	mov_2D_588	GTCACCATCAAGAGAGCTTGT	GCATGCATGTTGTATGCGCAA	Deletion Mapping
8	mov_2D_589	ACTAGCTATACGTTGAGCCGAT	TGGAGACGGCGACGACGAA	Deletion Mapping
9	TaWUS2D_full	ACCACCTTCTTCTTGCTGC	GGAGCACTCTCGGAGCAC	Deletion Mapping and TILLING
10	2D492200_F1	TCAGGCAGTAGTTCTCCCAAATA	TTCGAAGATTGTCGTCTTAAAGT	Deletion Mapping
11	2D492300_F1	ATTCGATGCTTTACCATTTTACA	CACAACAGCACAAAATGAGGC	Deletion Mapping
12	2D492400_F1	GCTGCTGACACGGATATACAGAT	GCACAGGCTATGCATACTGTTTA	Deletion Mapping
13	mov_2D_591	GGGGAACCACTTGTTTGACTA	TTTCGGATGGACGTAGTAATG	Deletion Mapping
14	mov_2D_592	AATGGAAGAACAAAGCCCCG	ACACCGAATGGCCAATGCGA	Deletion Mapping
15	mov_2D_593	GCCTTTTCGTAAGTTTGGGAGGT	AGGACTGCGAGGTGAGCGAA	Deletion Mapping
16	mov_2D_594	GTGTGTTGAAGAAGAAAGGTGTG	CTGTTTATCCTCTGCTGGTTCT	Deletion Mapping
17	mov_2D_595	AGATGTGTGTGCATTCTGGG	CGAACGAACAGGGTCCGCTG	Deletion Mapping
18	mov_2D_596	CGGTGCCCTCCATAAGTAAAC	CCCCAACCGTGGAATGTATTTA	Deletion Mapping
19	TaWUS2A_control	GCACCACCTGCCTTCTTC	CTCCCCAGCAAGTAGTAGTAGTG	Used as Control for Deletion Mapping
20	psaurus_mov_full	TTCCGTCCGAGTTAATATATACG	AAAATGTGTTGACTGGAAACTGA	Large Gene Fragment Cloning
21	tawus2D_tilling_1	TATATACCCGGCCTCTCACG	GAGCACTAGGCAAGGAGAGCTA	TILLING
22	tawus2D_tilling_2	ACGTCCTCCCTCTCTGTCG	GAGCACTCTCGGAGCACTAGG	TILLING

References

1. Alonge, M. *et al.* Automated assembly scaffolding using RagTag elevates a new tomato system for high-throughput genome editing. *Genome Biol* **23**, 258 (2022).
2. Li, H. Minimap2: pairwise alignment for nucleotide sequences. *Bioinformatics* **34**, 3094–3100 (2018).
3. Pérez-Wohlfeil, E., Diaz-del-Pino, S. & Trelles, O. Ultra-fast genome comparison for large-scale genomic experiments. *Sci Rep* **9**, 10274 (2019).
4. Altschul, S. F. *et al.* Gapped BLAST and PSI-BLAST: a new generation of protein database search programs. *Nucleic Acids Res* **25**, 3389–3402 (1997).
5. Li, H. *et al.* The Sequence Alignment/Map format and SAMtools. *Bioinformatics* **25**, 2078–2079 (2009).
6. Walkowiak, S. *et al.* Multiple wheat genomes reveal global variation in modern breeding. *Nature* **588**, 277–283 (2020).
7. Luo, M. C. *et al.* Genome sequence of the progenitor of the wheat D genome Aegilops tauschii. *Nature* **551**, 498–502 (2017).
8. Appels, R. *et al.* Shifting the limits in wheat research and breeding using a fully annotated reference genome. *Science (1979)* **361**, (2018).
9. Ramírez-González, R. H. *et al.* The transcriptional landscape of polyploid wheat. *Science (1979)* **361**, (2018).
10. Kim, D., Paggi, J. M., Park, C., Bennett, C. & Salzberg, S. L. Graph-based genome alignment and genotyping with HISAT2 and HISAT-genotype. *Nat Biotechnol* **37**, 907–915 (2019).
11. Brinton, J., Simmonds, J. & Uauy, C. Ubiquitin-related genes are differentially expressed in isogenic lines contrasting for pericarp cell size and grain weight in hexaploid wheat. *BMC Plant Biol* **18**, 22 (2018).
12. Danecek, P. *et al.* Twelve years of SAMtools and BCFtools. *Gigascience* **10**, (2021).
13. Liao, Y., Smyth, G. K. & Shi, W. The R package Rsubread is easier, faster, cheaper and better for alignment and quantification of RNA sequencing reads. *Nucleic Acids Res* **47**, e47–e47 (2019).
14. Robinson, M. D., McCarthy, D. J. & Smyth, G. K. edgeR: a Bioconductor package for differential expression analysis of digital gene expression data. *Bioinformatics* **26**, 139–140 (2010).
15. Love, M. I., Huber, W. & Anders, S. Moderated estimation of fold change and dispersion for RNA-seq data with DESeq2. *Genome Biol* **15**, 550 (2014).
16. Criscuolo, A. & Gribaldo, S. BMGE (Block Mapping and Gathering with Entropy): a new software for selection of phylogenetic informative regions from multiple sequence alignments. *BMC Evol Biol* **10**, 210 (2010).
17. Katoh, K. & Standley, D. M. MAFFT Multiple Sequence Alignment Software Version 7: improvements in performance and usability. *Mol Biol Evol* **30**, 772–780 (2013).
18. Lemoine, F. *et al.* NGPhylogeny.fr: new generation phylogenetic services for non-specialists. *Nucleic Acids Res* **47**, W260–W265 (2019).
19. Altschul, S. F., Gish, W., Miller, W., Myers, E. W. & Lipman, D. J. Basic local alignment search tool. *J Mol Biol* **215**, 403–410 (1990).
20. Letunic, I. & Bork, P. Interactive Tree of Life (iTOL) v6: recent updates to the phylogenetic tree display and annotation tool. *Nucleic Acids Res* **52**, W78–W82 (2024).

21. Huelsenbeck, J. P. & Ronquist, F. MRBAYES: Bayesian inference of phylogenetic trees. *Bioinformatics* **17**, 754–755 (2001).
22. Arora, S., Steed, A., Goddard, R. *et al.* A wheat kinase and immune receptor form host-specificity barriers against the blast fungus. *Nat. Plants* **9**, 385–392 (2023).
23. Sim, N.-L. *et al.* SIFT web server: predicting effects of amino acid substitutions on proteins. *Nucleic Acids Res* **40**, W452–W457 (2012).
24. Choi, Y. & Chan, A. P. PROVEAN web server: a tool to predict the functional effect of amino acid substitutions and indels. *Bioinformatics* **31**, 2745–2747 (2015).
25. Singh, N., Raupp, J., Koo, DH. *et al.* In-silico detection of aneuploidy and chromosomal deletions in wheat using genotyping-by-sequencing. *Plant Methods* **16**, 45 (2020).